JOURNAL OF THE ROYAL SOCIETY Interface

FirstCite® e-publishing

J. R. Soc. Interface
doi:10.1098/rsif.2012.0060
Published online

Effect of solid surface charge on the binding behaviour of a metal-binding peptide

Senem Donatan[1,2], Mehmet Sarikaya[3], Candan Tamerler[2,3,*] and Mustafa Urgen[1,*]

[1]*Department of Materials Science and Engineering, and* [2]*Molecular Biology, Biotechnology and Genetics Research Center (MOBGAM), Istanbul Technical University, Istanbul, Maslak 34469, Turkey*
[3]*Materials Science and Engineering, University of Washington, Seattle, WA 98195, USA*

Over the last decade, solid-binding peptides have been increasingly used as molecular building blocks coupling bio- and nanotechnology. Despite considerable research being invested in this field, the effects of many surface-related parameters that define the binding of peptide to solids are still unknown. In the quest to control biological molecules at solid interfaces and, thereby, tailoring the binding characteristics of the peptides, the use of surface charge of the solid surface may probably play an important role, which then can be used as a potential tuning parameter of peptide adsorption. Here, we report quantitative investigation on the viscoelastic properties and binding kinetics of an engineered gold-binding peptide, $3RGBP_1$, adsorbed onto the gold surface at different surface charge densities. The experiments were performed in aqueous solutions using an electrochemical dissipative quartz crystal microbalance system. Hydrodynamic mass, hydration state and surface coverage of the adsorbed peptide films were determined as a function of surface charge density of the gold metal substrate. Under each charged condition, binding of $3rGBP_1$ displayed quantitative differences in terms of adsorbed peptide amount, surface coverage ratio and hydration state. Based on the intrinsically disordered structure of the peptide, we propose a possible mechanism for binding of the peptide that can be used for tuning surface adsorption in further studies. Controlled alteration of peptide binding on solid surfaces, as shown here, may provide novel methods for surface functionalization used for bioenabled processing and fabrication of future micro- and nanodevices.

Keywords: solid-binding peptides; gold; metal surface charge; molecular recognition; adsorption

1. INTRODUCTION

Solid-binding peptides have been extensively exploited as molecular building blocks in nanoscale science and engineering in the last decades because of their material selective properties [1–3]. These short peptides (7–14 amino acids long) are commonly selected using biocombinatorial selection procedures, such as phage display [4,5] or cell-surface display [6–8]. Molecular biology and bioinformatics tools can be further applied to improve the solid-binding properties of the identified peptides [9,10]. Solid-binding peptides differentiate from other polypeptides with their specific molecular recognition properties onto targeted inorganic surfaces [1,11–13]. They have high affinity and specificity to their relevant inorganics with kinetic equilibrium constants in the range of 10^6–$10^7\,M^{-1}$ and negative binding energies in the vicinity of 8–9 kcal mole^{-1} [14–16]. Since their discovery, solid-binding peptides have been used successfully in myriad practical applications as synthesizers and growth modifiers in nanoparticle synthesis [17,18] or biomineralization processes [19,20], as molecular linkers and assemblers in targeted organization of functional hybrid nanostructures [11,21]. Despite to all these accomplishments, the intriguing relationship between solid-binding peptides and their associated solids has not been revealed clearly [22–25]. Elucidating the molecular recognition mechanisms will enable the control of interactions at the peptide–solid interface leading to the realization of peptide-based novel hybrid molecular technologies [11].

The efforts to elaborate the recognition mechanisms of solid-binding peptides have been focused mainly on structural (peptide conformation or solid surface configuration) [23,26] or physico-chemical interactions (short- and long-range forces, e.g. coulomb forces, van der Waals forces, dipole–dipole interactions, hydrogen bonding, etc.) [24,27,28]. The most important contributing factor

*Authors for correspondence (urgen@itu.edu.tr; candan@u.washington.edu).

Electronic supplementary material is available at http://dx.doi.org/10.1098/rsif.2012.0060 or via http://rsif.royalsocietypublishing.org.

Received 24 January 2012
Accepted 16 March 2012

in peptide binding to charged or polar solid surfaces is proposed as electrostatic interactions [2,29,30]. However, the quantitative contribution of coulomb forces to specific recognition at peptide–solid interface has not yet been fully investigated.

In this study, the effect of metal surface charge on the binding of an engineered gold-binding peptide (GBP) was analysed. GBP motif (MHGKTQATSG-TIQS) had been originally selected by cell-surface display and identified as one of the strongest binders within the other selected GBPs. By engineering this peptide in triple-repeated form ($3rGBP_1$), its binding affinity was further enhanced. The binding and assembly characteristics of $3rGBP_1$ have been studied in detail by our and other groups [21,23,31–33]. Here, time-dependent *in situ* adsorption experiments of $3rGBP_1$ were carried out by applying an external electrical field using electrochemical dissipative quartz crystal microbalance (EQCM-Z) system [34,35]. Charge density of the metal surface was altered by changing the external voltage at the metal–electrolyte interface. The viscoelastic nature of the adsorbed peptide films was followed via impedance monitoring. We first optimized the applied external voltage with respect to charge density at the gold–buffer and peptide–gold interfaces. Then viscoelastic properties and kinetic parameters of $3rGBP_1$ films were investigated as a function of gold surface charge. Finally, a charge-dependent binding behaviour model was proposed.

2. MATERIAL AND METHODS

2.1. Peptide, buffer and solutions

$3rGBP_1$ was synthesized using an automated solid-phase peptide synthesizer (CS336X, CSBio Inc., Menlo Park, CA). A standard Fmoc solid-phase peptide synthesis technique was employed. The N- or C-termini of the peptide were not blocked during synthesis. After synthesis, the peptide was purified by C-18 reverse-phase liquid chromatography to a level greater than 95 per cent. Peptide solutions were prepared in 10 mM phosphate buffer (3 : 1 K_2HPO_4–KH_2PO_4, containing 100 mM KCl) under various concentrations (200 nM, 500 nM, 800 nM, 1.2 µM). Maximum peptide concentration was chosen as 1.2 µM to ensure working in the monolayer range [32]. The pH of the buffer was adjusted to pH 7.4. All solutions were prepared using ultrapure water (Merck & Co, Inc., USA).

2.2. Quartz crystals

Crystals (KSV Instruments, Norway) coated with a thin polycrystalline gold layer were used. They have a fundamental frequency of 5 MHz, a constant factor of 17.7 ng $cm^{-2}Hz$ and a geometric area of 0.78 cm^2 gold working surface. Prior to the first use, crystals were rinsed with ultrapure water, dried under a stream of nitrogen and treated in a UV–ozone chamber for 10 min. For removal of organic films after peptide adsorption, crystals were introduced into UV–ozone for 20 min and then exposed into a NH_4OH (28%): H_2O_2 (30%): H_2O (1 : 1 : 5 v/v/v) mixture at 75°C for 5 min, and further cleaned in a UV–ozone chamber for 20 min.

2.3. Electrochemical quartz crystal microbalance experiments

A QCM-Z instrument (KSV Instruments, Norway) having a specially designed, temperature-controlled electrochemical flow cell module was used. The inner volume of the electrochemical flow cell was approximately 1.5 ml. A peristaltic pump (Ismatec SA, Switzerland) was used to introduce the desired solutions into the cell. The flow rate was kept at 100 µl min^{-1} for runs. The temperature was kept constant at 25°C. First, buffer solution was supplied into the system. After stabilization of the frequency, the desired potential was applied in the interval of [−0.4 to 0.4 V] versus normal hydrogen electrode (NHE) to the gold surface. For this purpose, a chronoamperometry technique was employed. Since polarization caused drift in the resonant frequency, frequency stabilization was required for each potential application step. Then 1.5 ml peptide solution with the desired concentration was fed to the system to allow binding. Next, sufficient buffer was introduced into the system to enable desorption of weakly bound peptides.

Changes in frequency and dissipation were recorded simultaneously associated with four overtone frequencies (15, 25, 35 and 45 MHz). These frequencies correlate with the third, fifth, seventh and ninth harmonics ($n = 3, 5, 7, 9$). In this report, frequency data from the third up to the ninth harmonics were used in the viscoelastic model. Normalized frequency shifts of the third harmonic were processed in the kinetic model.

For electrochemical measurements, QCM-Z was connected to a potentiostat (Compactstat, Ivium Technologies, The Netherlands). Measurements were conducted using a conventional three-electrode configuration. The gold-coated quartz crystals and a platinum disc were used as the working electrode and the counter electrode, respectively, and they were positioned parallel to each other. A small Dri-ref-2SH electrode (World Precision Instruments, UK) containing KCl gel (3 M KCl saturated Ag/AgCl pellets) served as the reference electrode, with a redox potential of −225 mV versus NHE at 25°C. All potentials reported in this paper were expressed with respect to NHE.

Cyclic voltammetry (CV) was performed to check the electrochemical stability interval of the metal surface in phosphate buffer with a potential scan rate of 50 mV s^{-1}. To assess the potential of zero charge (PZC) of the gold surface, differential capacitances at the gold–buffer interface were measured with AC impedance technique in buffer electrolytes with decreasing salt concentration [36]. Electrode potential-dependent impedance data (i.e. differential capacitance curve) were obtained by applying a frequency of 60 Hz and amplitude of 3 mV to the electrode, which was polarized, with a scan rate of 10 mV s^{-1}. Then, PZC was determined from the position of the diffuse layer minimum at the differential capacitance curve of 1 mM KCl containing electrolyte solution. Differential capacitance curves obtained in 100 mM KCl measurements

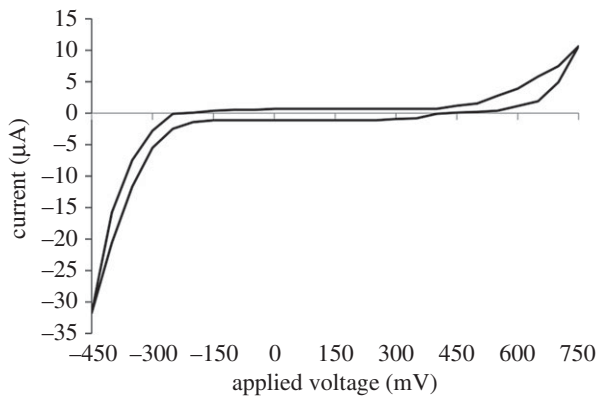

Figure 1. Cyclic voltammetry plot of the gold surface immersed in 100 mM KCl containing phosphate buffer at pH 7.4.

were used for determining the surface charge densities on gold at different potentials.

3. RESULTS AND DISCUSSIONS

3.1. The relation between applied potential and surface charge density at gold–buffer–peptide interface

Prior to conducting $3rGBP_1$ adsorption experiments, the potential application window free from Faradaic reactions was determined to eliminate any undesired reactions between the gold surface and the buffer electrolyte. CV data were recorded in 100 mM KCl containing phosphate buffer solution having a pH of 7.4 after degassing the electrolyte under vacuum. The region between −280 and 490 mV shows no evidence of Faradaic processes in figure 1. The increase in current at potentials higher than 490 and −280 mV is due to the dissociation of water and hydrogen evolution, respectively (figure 1). Thus, the system is electrochemically stable between −280 and 490 mV. The gold surface was polarized within this potential interval for preventing adsorption intervening electrochemical events on the gold surface.

Throughout $3rGBP_1$ adsorption studies, gold surfaces were polarized in positive and negative directions with respect to the open circuit potential (OCP = 73 ± 10 mV versus NHE) and frequency shifts obtained from EQCM-Z system were investigated. Maximum frequency shifts were assessed when the gold surface was polarized to −167 and 233 mV versus NHE in negative and positive directions, respectively. Thereafter, by shifting these potentials 100 mV in both directions; to −267 and 333 mV, a reduction in frequency gradients was observed when compared with OCP condition. Another experiment was also conducted at PZC of the gold surface that was determined from differential capacitance curve obtained in the buffer solution as 143 ± 10 mV versus NHE to define the charging state of the gold surface. Adsorption studies of $3rGBP_1$ at PZC showed a decrease in frequency shifts with respect to OCP condition.

Surface charge densities at corresponding applied potentials are presented in table 1 and the calculations

Table 1. Charge density (σ) of the gold surface at applied external voltages (mV). PZC and OCP refer to 143 ± 10 mV and 73 ± 10 mV, respectively.[a]

$V_{applied}$ (mV)	σ (μC cm^{-2})
333	13.60 ± 1.27
233	9.55 ± 0.73
PZC	0 ± 0.96
OCP	−3.03 ± 0.05
−167	−6.96 ± 0.32
−267	−11.17 ± 1.15

[a]The errors represent s.d.

for surface charge density are given in the electronic supplementary material. Results in table 1 indicate that the gold surface is negatively charged at OCP (standard binding condition for $3rGBP_1$). The results reported here demonstrate for the first time that the binding of the peptide at OCP occurs on the negatively charged gold surface. $3rGBP_1$ is known to have a high affinity to gold surface at this condition [23]. Thus, high affinity of $3rGBP_1$ at OCP could be related to the strong electrostatic attraction between cationic residues of $3rGBP_1$ and the negatively charged gold surface.

3.2. Viscoelastic properties of adsorbed $3rGBP_1$ films at different surface charges

In this part of the study, we monitored the viscoelastic nature of adsorbed peptide films via impedance changes using an EQCM-Z system. Basically, quartz crystal microbalance (QCM) is a very sensitive mass sensor, which detects deposited acoustic mass (hydrodynamic mass in liquid systems) [34]. In this technique, the resonant frequency is shifted depending on the amount of the mass (even in subnanogram ranges) deposited onto the surface of the quartz crystal. A decrease in frequency is related to the accumulated mass according to the well-known Sauerbrey equation [37]. However, the Sauerbrey equation is mostly valid for adsorption of rigid substances (e.g. solids and some gases). In liquids, adsorption of flexible biomolecules causes a shift in the resonance frequency and simultaneously a broadening in the resonant peak. This broadening stems from the energy dissipation (damping) not only between the adsorbed molecules but also among adsorbate and solute (mostly water) interactions [38]. These viscoelastic effects should be measured using dissipation [38] or impedance [39] monitoring and included in the calculations to obtain reliable results in liquids.

Frequency and dissipation shifts obtained from EQCM-Z system at several charge densities of the gold surface were fit to a viscoelastic model [39] (see also the electronic supplementary material). Concentration-dependent changes in hydrodynamic mass (peptide associated with water) of adsorbed $3rGBP_1$ films under different surface charges are presented in figure 2.

Results in figure 2 indicate that the adsorbed hydrodynamic peptide mass can be tuned by alteration of the gold surface charge. When compared with OCP (−3 μC cm^{-2}), an enhancement in adsorbed hydrated peptide amount was observed when the surface charge

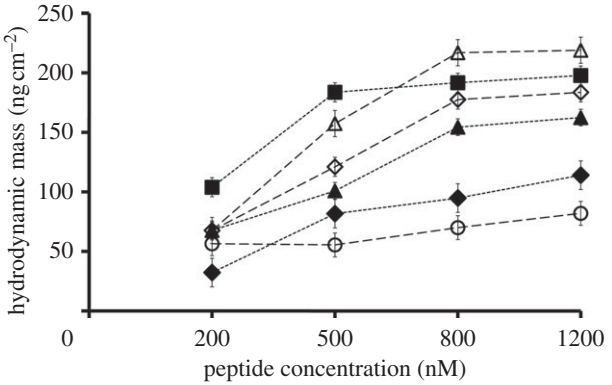

Figure 2. Concentration-dependent adsorbed hydrated 3rGBP$_1$ amounts under different surface charge densities of the gold surface (i–iii). (i) The error bars represent s.d. (ii) For simplicity, only integer values were shown for each different surface charge. (iii) Dashed lines indicate the trend at each condition. Filled diamonds, 13 μC cm^{-2}; filled squares, 9 μC cm^{-2}; filled triangles, 0 μC cm^{-2}; open diamonds, −3 μC cm^{-2}; open triangles, −7 μC cm^{-2}; open circles, −11 μC cm^{-2}.

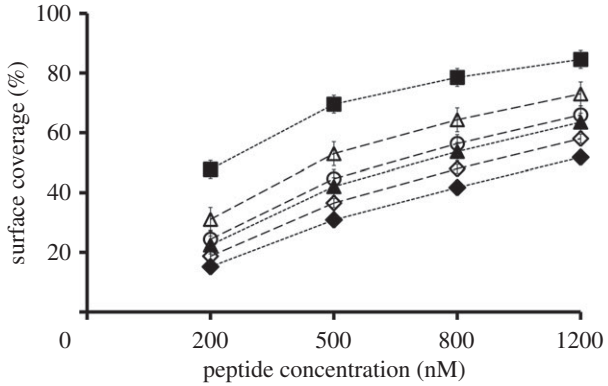

Figure 3. Concentration-dependent surface coverage of adsorbed hydrated 3rGBP$_1$ molecules under different charge densities of the gold surface. The error bars represent s.d. Filled diamonds, 13 μC cm^{-2}; filled squares, 9 μC cm^{-2}; filled triangles, 0 μC cm^{-2}; open diamonds, −3 μC cm^{-2}; open triangles, −7 μC cm^{-2}; open circles, −11 μC cm^{-2}.

is −7 and 9 μC cm^{-2}. Whereas by further increasing the surface charge both in negative and positive directions, i.e. −11 and 13 μC cm^{-2}, a reduction in adsorbed hydrated peptide amount was obtained.

3.3. Charge-dependent adsorption kinetics of 3rGBP$_1$

Adsorption kinetics of organic molecules can be directly measured by using QCM *in situ* under flow. To obtain kinetic parameters, resulting frequency shifts under charged conditions were fit to the modified two-step Langmuir adsorption model [32]. The modified model consists of a combination of 1 : 1 Langmuir [40] and two-state conformational change model [41]. Detailed interpretation of the model and the curve-fitting procedure are provided in the electronic supplementary material.

Ratios of the concentration-dependent surface coverage of adsorbed hydrodynamic peptide films at different surface charges are shown in figure 3. If 3rGBP$_1$ was a rigid substrate, maximum peptide coverage should have taken place with the maximum peptide amount adsorbed. However, in our case, the highest adsorbed peptide amount (figure 2) does not correlate with the maximum surface coverage (figure 3). This may be caused by the variation in the water-holding capacity as well as alteration in the conformation of the peptide at different charge densities on the gold surface.

3.3.1. Water-holding capacity of 3rGBP$_1$

Water may get trapped into the adsorbed 3rGBP$_1$ films owing to the conformationally flexible nature of the molecules. Since QCM measures the adsorbed molecular films coupled with water [42], we assumed that adsorbed peptide films incorporate a certain amount of water. Using the dynamic density results acquired from viscoelastic model for each charged surface condition, hydration ratios of the films (figure 4) were estimated for the highest peptide concentration (1.2 μM; see details in the supplementary material). Here, experiments conducted at −11 and 13 μC cm^{-2} charge densities were excluded, since they caused uncertainty in the viscoelastic model while analysing the dynamic density values.

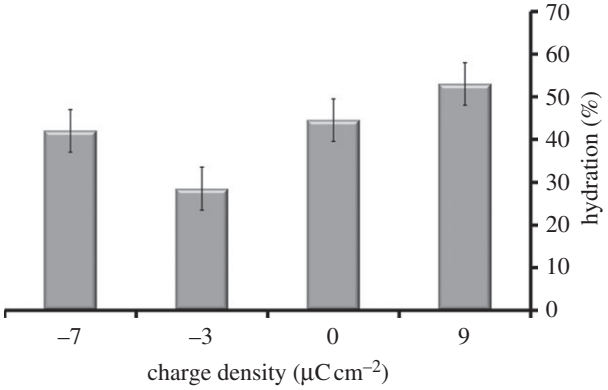

Figure 4. Hydration ratios of adsorbed 3rGBP$_1$ molecules using 1.2 μM peptide solution under several surface charges. The error bars represent s.d.

As indicated in figure 4, polarization alters the hydration of the adsorbed peptide films. Thus, water coupled to 3rGBP$_1$ at the interface might have contributed differently to molecular recognition under each charged condition. To understand this phenomenon in detail, covered areas of hydrated and dehydrated peptides were calculated at different surface charges (table 2) by using the data presented in figures 2–4.

When the surface charge density equals 9 μC cm^{-2}, more than half of the total covered area (0.351 in 0.666 cm^2) is held by the associated water molecules implying an excessive hydration of the peptides under this condition. Whereas the lowest hydration is observed at OCP condition (i.e. −3 μC cm^{-2}) since the residual area for coupled water is rather small in this case with regard to the total area covered by peptide and their associated water molecules (0.130 in 0.455 cm^2).

3.3.2. Conformational adaptation of 3rGBP$_1$

Viscoelastic and kinetic results demonstrate that 3rGBP$_1$ has the ability to adapt itself to each charged

Table 2. Surface coverage of hydrated and dehydrated $3rGBP_1$ molecules in 1.2 μM peptide solution at different surface charges.

σ (μC cm^{-2})	total area covered by hydrated peptides (cm^2)	area covered by dehydrated peptides (cm^2)	residual area for associated water (cm^2)
9	0.664	0.313	0.351
0	0.498	0.275	0.223
−3	0.455	0.325	0.130
−7	0.573	0.333	0.240

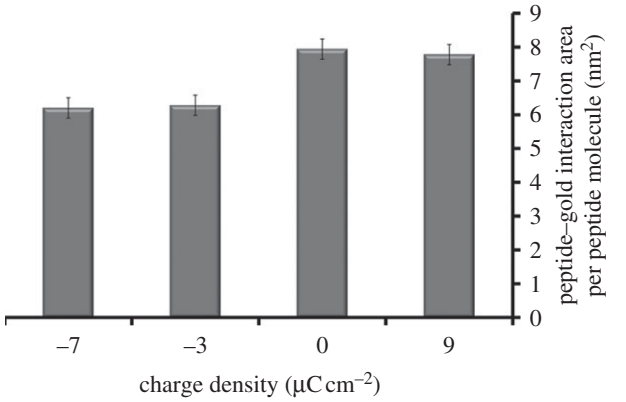

Figure 5. Maximum interaction area between a single $3rGBP_1$ molecule and the gold surface under several surface charge densities. The error bars represent s.d.

environment on the gold surface whether the excess surface charge is zero, negative or positive. In solutions with pH 7.4, $3rGBP_1$ consists of a single negatively charged residue on C-terminus, three positively charged lysine residues and several hydrophobic and partially negatively charged polar side chains [43]. Given the fact that $3rGBP_1$ has a flexible open linear conformation [23], charged or hydrophobic residues may easily be accessible on the peptide surface. Moreover, $3rGBP_1$ molecules are reported to be intrinsically disordered [23], which is a common feature for biomineralization proteins [26,44]. This behaviour may have enhanced the adaptation ability of $3rGBP_1$ molecules at different metal surface charge densities.

Unfortunately, it is not possible to detect conformational changes of $3rGBP_1$ molecules using EQCM-Z technique. At this point, maximum interaction area of a single $3rGBP_1$ molecule on gold may give additional physical insight for binding characteristics of the adsorbed peptides; whether the peptides are oriented in a stretched or condensed structure on the surface. Surely, it does not mean that the all peptide molecules will have the same structure on the surface but this might provide us with an idea of the conformation of the average peptide population adsorbed on the gold surface. For this purpose, the number of adsorbed peptide molecules per covered area was calculated for each charged surface condition. Taking into account corresponding surface coverage of $3rGBP_1$ films, the maximum area covered by an individual peptide molecule on the surface was further estimated under different charge densities (figure 5).

Previous NMR studies revealed that the dimensions of one $3rGBP_1$ molecule are $1 \times 2 \times 4$ nm [32]. Based on this finding, we assumed the largest possible interaction area for one $3rGBP_1$ molecule on gold surface as approximately 8 nm^2. Interestingly, results obtained at different surface charge densities (0 and 9 μC cm^{-2}) are found to be very close to the largest possible peptide–gold interaction area for one molecule (figure 5). Thus, under these conditions, peptides are most probably oriented on the gold surface by making the largest possible contact with the underlying gold surface. Under the negatively charged gold surfaces, i.e. at −3 and −7 μC cm^{-2}, peptide–gold interaction area for a single molecule reduces to 6 ± 0.5 nm. As a consequence, the conformation of the peptides probably changes by decreasing their contact area with the surface.

3.4. *Proposed charge-dependent binding behaviour of 3rGBP$_1$ on gold*

Based on the data given in table 2 and figure 5, one possible binding behaviour for $3rGBP_1$ was proposed under the analysed charged conditions at equilibrium (figure 6).

When the excess surface charge on gold was zero (i.e. PZC condition), the maximum peptide–gold interaction area obtained correlates with the largest possible interaction area for a single $3rGBP_1$ molecule. Therefore, we suggest that $3rGBP_1$ molecules most probably oriented on the gold surface using their largest surface area, i.e. in their extended form (figure 6*b*). Here, the electrostatic interactions between the gold surface and the peptide molecules should be at minimum, and therefore hydrophobic interactions are expected to be thermodynamically more favourable [45]. Thus, peptides may prefer to attach to the gold surface through their hydrophobic residues.

When compared with zero charge conditions, excess positive charge (9 μC cm^{-2}) on the gold surface may have increased both the available adsorption sites and also the hydrated state of the peptides but probably not the peptide conformation (figure 6*c*). According to the results in figure 5, the observed maximum peptide–gold interaction area under this condition is yet again very close to the largest possible interaction area for one $3rGBP_1$ molecule implying possibly a stretched orientation of $3rGBP_1$ on the gold surface. While there is electrostatic repulsion between positively polarized gold surface and the positively charged lysine residues along the peptide's backbone, the abundance of repeating partially negatively charged polar residues may have led to repeating local electrostatic attractions between $3rGBP_1$ molecules and the gold surface. Peptide recognition occurring via polar residues may have caused an enhanced accumulation of water molecules at peptide–gold interface. The maximum hydration state of the peptides assessed under this condition (figure 4) supports our suggestion.

Excess negative charge (−3 μC cm^{-2}, i.e. OCP condition) caused a reduction in the area of interaction at the peptide–gold interface for a single-peptide molecule (figure 5) when compared with the excess positive and zero net-charged conditions. Peptides are probably

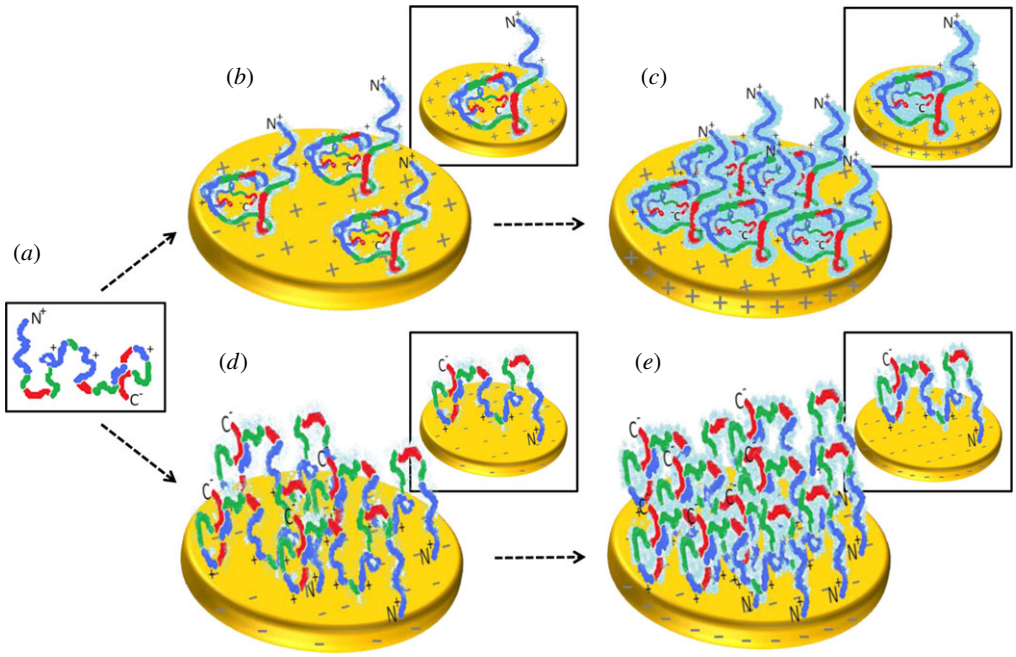

Figure 6. (*a*) Predicted conformation of $3rGBP_1$ in bulk solution at pH 7.4 based on reported theoretical modelling studies (adapted from So *et al.* [23]). Proposed binding behaviour of $3rGBP_1$ on gold substrate under equilibrium conditions at various surface charge densities; (*b*) 0, (*c*) 9, (*d*) −3, (*e*) $-7\ \mu C\ cm^{-2}$, respectively. Suggested potential orientation of $3rGBP_1$ at related gold surface charges are given in insets. Colours in the molecular structure of the peptide represent corresponding amino acid side chains as red refers to polar and anionic, dark blue refers to cationic and green refers to hydrophobic residues. Light blue represents the water molecules held by peptides.

decreasing their contact area with the gold surface. Additionally, water-holding capacity diminishes significantly under this condition (table 2). Here, the electrostatic attraction between the positively charged lysine residues and the negatively charged gold surface may have become dominant, while the polar residues on the peptide's backbone may have become less accessible at the gold–solution interface (figure 6*d*). Our proposal based on the experimental findings support the previous theoretical modelling studies [23], which claim that $3rGBP_1$ molecules form polypod structures, probably attaching to the surfaces through their positively charged residues. We believe that this is a unique contribution in linking experimental findings to theoretical findings.

Based on the results in table 2 and figure 5, increase in excess negative charge ($-7\ \mu C\ cm^{-2}$) led to an increase in the adsorbed amount and water-holding capacity of the peptides but not a significant change in the peptide orientation when compared with OCP condition (figure 6*e*). Under this condition, we again propose a dense peptide adsorption via lysine residues since the peptide conformation does not change significantly when compared with OCP condition (figure 5). Indeed, to uncover the interactions at the molecular scale, it would be very interesting to conduct molecular modelling studies under charged surface conditions.

Under the excess negative and positive charges (greater than $\pm 10\ \mu C\ cm^{-2}$), adsorbed peptide amounts decreased considerably when compared with OCP condition (figure 2). High positive surface charge density probably cause the conduction electrons to recede into the metal by forming a hard wall of metal ions [46], which may inhibit the adsorbate–solid surface interactions occurring at the interface. If the metal surface is highly polarized by excess negative charge, solvated cations can be attracted to the surface and accumulated in high amounts within the double layer [47]. This accumulation may also restrict the adsorbate–solid surface interaction. These findings reveal that the density of excess metal surface charge may be used as a key parameter in tuning the adsorption and binding properties of $3rGBP_1$.

4. CONCLUSIONS

In the literature, there are a number of studies where electrostatic interactions are proposed as the most likely reason for strong binding of solid-binding peptides to their relevant solids [2,29,30]. This study is the first experimental attempt in which the effect of metal surface charge was probed for the molecular recognition of a metal-binding peptide. Here, we report quantitative data about the viscoelastic properties and the binding kinetics of a GBP adsorbed onto the gold surface at different surface charge densities.

Results reveal that excess negative charge on the gold surface plays an important role in the binding properties of $3rGBP_1$ under non-polarized conditions. On polarized gold surfaces, $3rGBP_1$ adapted its adsorption to each charged environment whether the excess surface charge was zero, negative or positive, probably because of its conformational flexibility. Under each charged condition, binding behaviour of $3rGBP_1$ demonstrated quantitative differences in terms of adsorbed peptide amount, surface coverage ratio and hydration state.

The distinctive adsorption behaviour of $3rGBP_1$ on gold surface provides a way to tune the peptide

binding by varying the metal surface charge. The ability to alter the peptide binding on surfaces in a controllable and predictable way will extend the applicability of peptides as molecular linkers and/or couplers on bioenabled surface functionalization. Our results reveal that the density of induced charge is at least one of the key parameters to tune the binding of self-assembled peptides, unique potential utility in bio- and nanotechnological applications.

This work was mainly supported by the Turkish State Planning Organization via Advanced Technologies in Engineering and Scientific Research Unit at Istanbul Technical University. Partial support (M.S. and C.T.) was provided by Genetically Engineered Materials Science and Engineering Center supported by NSF through the MRSEC Programme and TUBITAK/NSF-IRES project (contract grant no. 107T250). S.D. thank Z. B. Akinci and B. D. Polat for their valuable comments while preparing the manuscript.

REFERENCES

1 Sarikaya, M., Tamerler, C., Jen, A. K. Y., Schulten, K. & Baneyx, F. 2003 Molecular biomimetics: nanotechnology through biology. *Nat. Mater.* **2**, 577–585. (doi:10.1038/nmat964)
2 Baneyx, F. & Schwartz, D. T. 2007 Selection and analysis of solid-binding peptides. *Curr. Opin. Biotechnol.* **18**, 312–317. (doi:10.1016/j.copbio.2007.04.008)
3 Whyburn, G. P., Li, Y. & Huang, Y. 2008 Protein and protein assembly based material structures. *J. Mater. Chem.* **18**, 3755–3762. (doi:10.1039/b807421f)
4 Kriplani, K. & Kay, B. K. 2005 Selecting peptides for use in nanoscale materials using phage-displayed combinatorial peptide libraries. *Curr. Opin. Biotechnol.* **16**, 470–475. (doi:10.1016/j.copbio.2005.07.001)
5 Donatan, S., Yazici, H., Bermek, H., Sarikaya, M., Tamerler, C. & Urgen, M. 2009 Physical elution in phage display selection of inorganic-binding peptides. *Mater. Sci. Eng. C* **29**, 14–19. (doi:10.1016/j.msec.2008.05.003)
6 Wittrup, K. D. 2001 Protein engineering by cell-surface display. *Curr. Opin. Biotechnol.* **12**, 395–399. (doi:10.1016/S0958-1669(00)00233-0)
7 Brown, S. 1997 Metal-recognition by repeating polypeptides. *Nat. Biotechnol.* **15**, 269–272. (doi:10.1038/nbt0397-269)
8 Peelle, B. R., Krauland, E. M., Wittrup, K. D. & Belcher, A. M. 2005 Probing the interface between biomolecules and inorganic materials using yeast surface display and genetic engineering. *Acta Biomater.* **1**, 145–154. (doi:10.1016/j.actiobio.2004.11.004)
9 Oren, E. E., Tamerler, C., Sahin, D., Hnilova, M., Seker, U. O. S., Sarikaya, M. & Samudrala, R. 2007 A novel knowledge-based approach to design inorganic-binding peptides. *Bioinformatics* **23**, 2816–2822. (doi:10.1093/bioinformatics/btm436)
10 Shiba, K. 2010 Natural and artificial peptide motifs: their origins and the application of motif-programming. *Chem. Soc. Rev.* **39**, 117–126. (doi:10.1039/b719081f)
11 Tamerler, C. & Sarikaya, M. 2009 Genetically designed peptide-based molecular materials. *ACS Nano* **3**, 1606–1615. (doi:10.1021/nn900720g)
12 Wei, Y. & Latour, R. A. 2009 Benchmark experimental data set and assessment of adsorption free energy for peptide–surface interactions. *Langmuir* **25**, 5637–5646. (doi:10.1021/la8042186)
13 Weiger, M. C., Park, J. J., Roy, M. D., Stafford, C. M., Karim, A. & Becker, M. L. 2010 Quantification of the binding affinity of a specific hydroxyapatite binding peptide. *Biomaterials* **31**, 2955–2963. (doi:10.1016/j.biomaterials.2010.01.012)
14 Tamerler, C., Oren, E. E., Duman, M., Venkatasubramanian, E. & Sarikaya, M. 2006 Adsorption kinetics of an engineered gold binding peptide by surface plasmon resonance spectroscopy and a quartz crystal microbalance. *Langmuir* **22**, 7712–7718. (doi:10.1021/la0606897)
15 Seker, U. O. S., Wilson, B., Dincer, S., Kim, I. W., Oren, E. E., Evans, J. S., Tamerler, C. & Sarikaya, M. 2007 Adsorption behavior of linear and cyclic genetically engineered platinum binding peptides. *Langmuir* **23**, 7895–7900. (doi:10.1021/la700446g)
16 Sano, K. I., Sasaki, H. & Shiba, K. 2005 Specificity and biomineralization activities of Ti-binding peptide-1 (TBP-1). *Langmuir* **21**, 3090–3095. (doi:10.1021/la047428m)
17 Li, Y., Whyburn, G. P. & Huang, Y. 2009 Specific peptide regulated synthesis of ultrasmall platinum nanocrystals. *J. Am. Chem. Soc.* **131**, 15 998–15 999. (doi:10.1021/ja907235v)
18 Coppage, R., Slocik, J. M., Sethi, M., Pacardo, D. B., Naik, R. R. & Knecht, M. R. 2010 Elucidation of peptide effects that control the activity of nanoparticles. *Angew. Chem. Int. Ed.* **49**, 3767–3770. (doi:10.1002/anie.200906949)
19 Yuca, E., Yazgan-Karatas, A., Seker, U. O. S., Gungormus, M., Dinler-Doganay, G., Sarikaya, M. & Tamerler, C. 2011 *In vitro* labeling of hydroxyapatite minerals by an engineered protein. *Biotech. Bioeng.* **108**, 1021–1030. (doi:10.1002/bit.23041)
20 Zhou, W., Schwartz, D. T. & Baneyx, F. 2010 Single-pot biofabrication of zinc sulfide immune-quantum dots. *J. Am. Chem. Soc.* **132**, 4731–4738. (doi:10.1021/ja909406n)
21 Hwang, L., Chen, C. L. & Rosi, N. L. 2011 Preparation of 1-D nanoparticle superstructures with tailorable thicknesses using gold-binding peptide conjugates. *Chem. Commun.* **47**, 185–187. (doi:10.1039/c0cc02257h)
22 Notman, R., Oren, E. E., Tamerler, C., Sarikaya, M., Samudrala, R. & Walsh, T. R. 2010 Solution study of engineered quartz binding peptides using replica exchange molecular dynamics. *Biomacromolecules* **11**, 3266–3274. (doi:10.1021/bm100646z)
23 So, C. R., Kulp, J. L., Oren, E. E., Zareie, H., Tamerler, C., Evans, J. S. & Sarikaya, M. 2009 Molecular recognition and supramolecular self-assembly of a genetically engineered gold binding peptide on Au{111}. *ACS Nano* **3**, 1525–1531. (doi:10.1021/nn900171s)
24 Evans, J. S. 2008 'Tuning in' to mollusk shell nacre- and prismatic-associated protein terminal sequences. Implications for biomineralization and the construction of high performance inorganic–organic composites. *Chem. Rev.* **108**, 4455–4462. (doi:10.1021/cr078251e)
25 Diamanti, S., Elsen, A., Naik, R. & Vaia, R. 2009 Relative functionality of buffer and peptide in gold nanoparticle formation. *J. Phys. Chem. C* **113**, 9993–9997. (doi:10.1021/jp8102063)
26 Evans, J. S., Samudrala, R., Walsh, T. R., Oren, E. E. & Tamerler, C. 2008 Molecular design of inorganic-binding polypeptides. *MRS Bull.* **33**, 514–518. (doi:10.1557/mrs2008.103)
27 Feng, J., Pandey, R. B., Berry, R. J., Farmer, B. L., Naik, R. R. & Heinz, H. 2011 Adsorption mechanism of single amino acid and surfactant molecules to Au {111} surfaces in aqueous solution: design rules for metal-binding

molecules. *Soft Matter* **7**, 2113–2120. (doi:10.1039/c0sm01118e)
28 Skelton, A. A., Liang, T. & Walsh, T. R. 2009 Interplay of sequence, conformation, and binding at the peptide–titania interface as mediated by water. *ACS Appl. Mater. Interface* **1**, 1482–1491. (doi:10.1021/am9001666)
29 Heinz, H., Jha, K. C., Luettmer-Strathmann, J., Farmer, B. L. & Naik, R. R. 2011 Polarization at metal–biomolecular interfaces in solution. *J. R. Soc. Interface* **8**, 220–232. (doi:10.1098/rsif.2010.0318)
30 Oren, E. E., Notman, R., Kim, I. W., Evans, J. S., Walsh, T. R., Samudrala, R., Tamerler, C. & Sarikaya, M. 2010 Probing the molecular mechanisms of quartz-binding peptides. *Langmuir* **26**, 11 003–11 009. (doi:10.1021/la100049s)
31 Park, T. J. *et al.* 2006 Protein nanopatterns and biosensors using gold binding polypeptide as a fusion partner. *Anal. Chem.* **78**, 7197–7205. (doi:10.1021/ac060976f)
32 So, C. R., Tamerler, C. & Sarikaya, M. 2009 Adsorption, diffusion, and self-assembly of an engineered gold-binding peptide on Au (111) investigated by atomic force microscopy. *Angew. Chem. Int. Ed.* **48**, 5174–5177. (doi:10.1002/anie.200805259)
33 Verde, A. V., Acres, J. M. & Maranas, J. K. 2009 Investigating the specificity of peptide adsorption on gold using molecular dynamics simulations. *Biomacromolecules* **10**, 2118–2128. (doi:10.1021/bm9002464)
34 Edvardsson, M., Svedhem, S., Wang, G., Richter, R., Rodahl, M. & Kasemo, B. 2009 QCM-D and reflectometry instrument: applications to supported lipid structures and their biomolecular interactions. *Anal. Chem.* **81**, 349–361. (doi:10.1021/ac801523w)
35 Van De Keere, I., Svedhem, S., Hogberg, H., Vereecken, J., Kasemo, B. & Hubin, A. 2009 *In situ* control of the oxide layer on thermally evaporated titanium and lysozyme adsorption by means of electrochemical quartz crystal microbalance with dissipation. *ACS Appl. Mater. Interface* **1**, 301–310. (doi:10.1021/am800029y)
36 Lipkowski, J. & Stolberg, L. 1992 Molecular adsorption at gold and silver electrodes. In *Adsorption of molecules at metal electrodes* (eds J. Lipkowski & P. N. Ross), ch. 1. New York, NY: VCH Publisher.
37 Sauerbrey, G. 1959 Verwendung von Schwingquarzen zur Wägung dünner Schichten und zur Mikrowägung. *Z. Phys.* **155**, 206–222. (doi:10.1007/BF01337937)
38 Hook, F., Kasemo, B., Nylander, T., Fant, C., Sott, K. & Elwing, H. 2001 Variations in coupled water, viscoelastic properties, and film thickness of a Mefp-1 protein film during adsorption and cross-linking: a quartz crystal microbalance with dissipation monitoring, ellipsometry, and surface plasmon resonance study. *Anal. Chem.* **73**, 5796–5804. (doi:10.1021/ac0106501)
39 Viitala, T. 2008 *Modelling with dissipative QCM, application notes*. Helsinki, Finland: KSV Instrument Ltd.
40 Karpovich, D. S. & Blanchard, G. J. 1994 Direct measurement of the adsorption-kinetics of alkanethiolate self-assembled monolayers on a microcrystalline gold surface. *Langmuir* **10**, 3315–3322. (doi:10.1021/la00021a066)
41 Yowler, B. C. & Schengrund, C. L. 2004 Botulinum neurotoxin A changes conformation upon binding to ganglioside GT1b. *Biochemistry* **43**, 9725–9731. (doi:10.1021/bi0494673)
42 Hook, F. *et al.* 2002 A comparative study of protein adsorption on titanium oxide surfaces using *in situ* ellipsometry, optical waveguide lightmode spectroscopy, and quartz crystal microbalance/dissipation. *Coll. Surf. B: Biointerfaces* **24**, 155–170. (doi:10.1016/S0927-7765(01)00236-3)
43 Berg, J. M., Tymoczko, J. L. & Stryer, L. 2006 *Biochemistry: international edition*, New York, NY: W. H. Freeman & Co. Ltd.
44 Delak, K., Collino, S. & Evans, J. S. 2009 Polyelectrolyte domains and intrinsic disorder within the prismatic asprich protein family. *Biochemistry* **48**, 3669–3677. (doi:10.1021/bi900113v)
45 Norde, W. 1986 Adsorption of proteins from solution at the solid–liquid interface. *Adv. Coll. Interface Sci.* **25**, 267–340. (doi:10.1016/0001-8686(86)80012-4)
46 Lipkowski, J. & Ross, P. N. 1993 *Structure of electrified interfaces*. New York, NY: VCH Publisher.
47 Bockris, J. O. & Reddy, A. K. N. 1970 *Modern electrochemistry: fundamentals of electrodics*, vol. 2, ch. 7. New York, NY: Kluwer/Plenum Press.